Amphiphilic Random Glycopolymer Based on Phenylboronic Acid: Synthesis, Characterization, and Potential as Glucose-Sensitive Matrix

ARTICLE *in* BIOMACROMOLECULES · MAY 2009

Impact Factor: 5.75 · DOI: 10.1021/bm8010006 · Source: PubMed

8 AUTHORS, INCLUDING:

Xinge Zhang
Nankai University
58 PUBLICATIONS **981** CITATIONS
SEE PROFILE

Xuejiao Zhang
Freie Universität Berlin
13 PUBLICATIONS **232** CITATIONS
SEE PROFILE

Zhen Wang
Nankai University
19 PUBLICATIONS **571** CITATIONS
SEE PROFILE

Chaoxing Li
Nankai University
55 PUBLICATIONS **873** CITATIONS
SEE PROFILE

Amphiphilic Random Glycopolymer Based on Phenylboronic Acid: Synthesis, Characterization, and Potential as Glucose-Sensitive Matrix

Xingju Jin,[†] Xinge Zhang,[*,†] Zhongming Wu,[‡] Dayong Teng,[†] Xuejiao Zhang,[†] Yanxia Wang,[†] Zhen Wang,[†] and Chaoxing Li[*,†]

Key Laboratory of Functional Polymer Materials of Ministry Education, Institute of Polymer Chemistry, Nankai University, Tianjin 300071, China, and Metabolic Diseases Hospital, Tianjin Medical University, Tianjin 300070, China

Received September 7, 2008; Revised Manuscript Received March 11, 2009

This study is devoted to developing amphiphilic, random glycopolymers based on phenylboronic acid, which self-assemble to form nanoparticles (NPs), as a glucose-sensitive agent. Maleimide-glucosamine was copolymerized with 3-acryl aminophenylboronic acid in methanol at 70 °C. Using the nanoprecipitation method, NPs with a narrow size distribution were successfully generated. Transmission electron microscopic analysis showed that the NPs were well dispersed as individual, spherically shaped particles. The swelling behavior of the NPs and the in vitro release profiles of insulin at different glucose concentrations revealed definite glucose sensitivity of the glycopolymers. Further, circular dichroism spectroscopy demonstrated that the overall tertiary structure of the released insulin was not altered compared with standard insulin. The analysis of relative cell proliferation suggested that the glycopolymer NPs had good biocompatibility. The glycopolymers that responded to changes in the glucose concentration of the surrounding environment are being aimed for use in self-regulated insulin delivery.

1. Introduction

Stimuli-responsive polymers (also known as "smart" polymers or "intelligent" polymers) have gained major scientific interest in different areas, for instance, drug delivery, diagnostics, chemical memory units, intelligent switches, and sensors.[1−5] These polymers undergo quick, reversible microstructure changes when exposed to external stimuli such as changes in pH,[6,7] temperature,[8−10] light,[11] ionic strength,[12] and magnetic field.[13] One of the most interesting and most investigated stimuli-responsive materials is the polymer bearing phenylboronic acid that responds to glucose in the surrounding environment.[14−18]

A significant problem in the treatment of insulin-dependent diabetes mellitus is the difficulty in controlling the insulin dosage. An overdose of insulin causes an excessive decrease in blood sugar that may lead to serious hypoglycemia. It would be most desirable for drug release to match a patient's physiological needs at the proper time and/or the proper site. The development of a glucose-responsive polymer that would allow for the construction of a self-regulated insulin delivery system would be a significant breakthrough in the treatment of diabetes.

Due to the specific and reversible interaction with diols, polyols, sugars, and glycoproteins, phenylboronic acid-functionalized polymeric materials have been developed for carbohydrate recognition, specific detection, and affinity chromatography, as well as drug delivery.[19−22] An important property of phenylboronic acid compounds in an aqueous medium is that they are in equilibrium between an uncharged and a charged form.[19] Only charged phenylborates can form a stable complex with glucose. Increasing glucose concentration increases the charged phenylborates, thus, enhancing the hydrophilicity of amphiphilic polymers having pendant phenylborate moieties.[23]

A number of studies investigating glucose-sensitive polymers have been reported and most are based on *N*-isopropylacrylamide and aminophenylboronic acid.[24−29] Hoare et al.[25] described glucose-responsive, thermosensitive gel NPs that could bind insulin by matching the charge profiles of insulin and the gel network at a proper pH. These NPs released insulin via a glucose-induced "on−off" switching of electrostatic attractions between insulin and the microgel.[25] Lapeyre et al.[27] also synthesized new multiresponsive, core−shell microgels that were used to encapsulate insulin and its release was regulated by the presence of glucose. Additionally, Zhang et al.[28] have investigated the volume phase transition of poly(*N*-isopropylacrylamide-phenylboronic acid) microgels in the presence of glucose and the effects of pH, ionic strength, and phenylboronic acid content on the glucose sensitivity of these gels.[28]

However, a disadvantage of boronic acid-containing compounds is that they have some degree of cytotoxic activity.[30,31] To address this problem, it is necessary to introduce biocompatible compounds. Carbohydrate-immobilized materials, which play an important role in a variety of biological phenomena, have recently attracted great interest due to their biological functions.[32−36] Additionally, the abundant hydroxyl groups of carbohydrates are responsible for both the hydrophilicity and biocompatibility of the carbohydrate-immobilized materials.[37−40]

Polymers containing carbohydrate moieties as pendant groups have received increasing attention as a "smart", artificial material, applicable for a variety of potential applications in biological and biomedical research.[41] Synthetic glycopolymers are expected to mimic, or even exceed, the performance of natural polysaccharides in specific applications. In the present paper, we synthesized glucose-responsive glycopolymers comprised of a phenylboronic acid-functionalized monomer (AAP-

* To whom correspondence should be addressed. Tel.: +86-22-23501645. Fax: +86-22-23505598. E-mail: zhangxinge@nankai.edu.cn (X.Z.); lcx@nankai.edu.cn (C.L.).
[†] Nankai University.
[‡] Tianjin Medical University.

10.1021/bm8010006 CCC: $40.75
Published on Web 04/27/2009

Scheme 1. Synthesis of the Random Amphiphilic Glycopolymer p(AAPBA-*r*-MAGA)

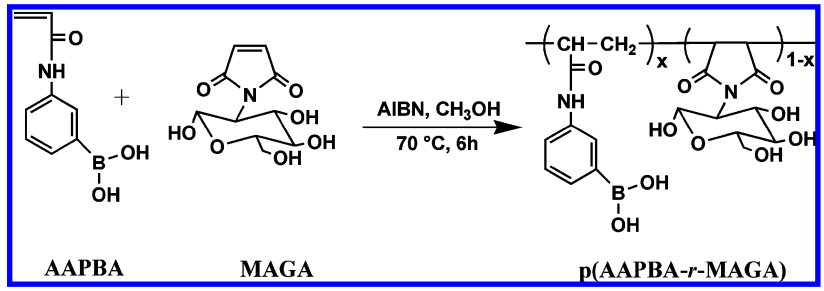

BA) and a glucosamine-carrying monomer (MAGA) using free-radical polymerization without any protection and deprotection procedure (Scheme 1). The glucose-responsive moieties were provided by AAPBA, while MAGA was introduced to improve the biocompatibility of the polymers. The obtained polymers were amphiphilic glycopolymers with random compositions of the two monomers. Although the great majority of reports[42−45] on self-assemblies are for well-defined block copolymers, some chemists have made an effort to explore if it is possible to form nanoassemblies from a random amphiphilic copolymer solution and have achieved an optimistic result.[46] The goal of the present work was to evaluate the self-assembling formation of NPs from synthesized glycopolymers and to investigate the in vitro release of the model drug, insulin, in response to changes in the concentration of glucose.

2. Experimental Section

2.1. Materials. 3-Aminophenylboronic acid monohydrate was purchased from Nanjing Kangmanlin Chemical Industry Co. Ltd. (Nanjing, China). Acryloyl chloride was prepared by refluxing acrylic acid and thionyl chloride for 8 h at 90 °C in our laboratory and freshly distilled before use. D-Glucosamine hydrochloride was purchased from the Shanghai No. 2 Reagent Factory. Maleic anhydride and D-glucose were supplied by the Tianjin No. 2 Chemical Reagent Factory. Sodium methoxide was synthesized according to the published procedure.[47] 2,2′-Azobisisobutyronitrile (AIBN, from Fluka) was recrystallized twice from ethanol and dried in a vacuum (mp 104 °C). Pure crystalline porcine insulin (with a nominal activity of 28 IU/mg) was obtained from Xuzhou Wanbang Biochemical Co. Ltd. (Jiangsu, China) and used without further purification. 3-[4,5-Dimethylthiazol-2-yl]-2,5-diphenyltetrazolium bromide (MTT) was purchased from the J & K China Chemical Ltd. (Beijing, China). The semipermeable membrane (molecular weight cutoff (MWCO) = 3500) used for dialysis was purchased from Shanghai Green Bird Science and Technology Co. Ltd. (Shanghai, China). All other chemicals were of analytical grade.

2.2. Preparation of AAPBA. AAPBA was prepared according to the method described by Lee et al.[48] Briefly, 3-aminophenylboronic acid monohydrate (5.0 g, 32.2 mmol) was dissolved in 40 mL of sodium hydroxide (5.16 g, 129.04 mmol) solution and cooled in an ice bath. Freshly distilled acryloyl chloride (3.2 mL, 40.0 mmol) was added dropwise to the 3-aminophenylboronic acid solution, while stirring, over a period of 30 min. After cooling to room temperature, the reaction mixture was stirred for a further 2 h. The pH of the mixture was adjusted to a pH = 8 using dilute HCl (0.1 M). The resulting beige precipitate was filtered and washed five times with 25 mL of cold water. The precipitate was dissolved in 80 mL of distilled water after heating to 80 °C, and the residual insoluble impurities were filtered off. The filtrate was left to stand overnight in a refrigerator, and the resulting crystals were filtered, crushed, and left to dry in a desiccator. The yield of AAPBA was 45%.

2.3. Preparation of MAGA. MAGA was synthesized by adapting the procedure previously reported by Aly et al.[49] D-Glucosamine hydrochloride (2.0 g, 9.27 mmol) and sodium methoxide (0.5 g, 9.26 mmol) were added to absolute methanol (25 mL) while stirring. The mixture was treated with maleic anhydride (0.46 g, 4.69 mmol) and stirred at 60 °C for 30 min. Then, Et_3N (0.93 mL) was added and the reaction mixture was again treated with maleic anhydride (0.46 g, 4.69 mmol). After stirring for 2 h at 60 °C, the solution was filtered and the filtrate was evaporated at reduced pressure to a viscous syrup. The syrup was added to excessive ethyl acetate, and the resulting dust-colored precipitate was filtered and rapidly collected to avoid absorbing moisture. The remaining solvent was removed under vacuum for 2 days to yield 1.9 g of MAGA (yield 79%).

Table 1. Copolymerization of AAPBA and MAGA

	monomer feed ratio (mol/mol)		composition[a] (mol/mol)		
sample	AAPBA	MAGA	AAPBA	MAGA	yield (%)
p(AAPBA1-*r*-MAGA1)	1	1	2.1	1	50 ± 2
p(AAPBA2-*r*-MAGA1)	2	1	2.7	1	58 ± 3
p(AAPBA4-*r*-MAGA1)	4	1	4.1	1	51 ± 2

[a] The composition of the glycopolymers was the approximate value calculated from the integral intensity of the ^{1}H NMR spectrum.

2.4. Copolymerization of AAPBA and MAGA. Briefly, AAPBA and MAGA were added to anhydrous methanol in a three-necked, round flask equipped with a reflux condenser, a nitrogen inlet and a thermometer. After purging N_2 for 30 min, copolymerization was initiated by AIBN (5% molar of the total monomers). The stirring solution was closed in a nitrogen atmosphere at 70 °C. The copolymerization was continued for 6 h and the precipitated copolymer was filtered and washed with excess methanol. The obtained copolymer was dried under a vacuum at 60 °C. The yield was calculated by the mass ratio of the glycopolymer product to the total monomers in the feed. By changing the feed molar ratio of AAPBA to MAGA (1:1, 2:1 and 4:1), three distinct glycopolymers were obtained. For simplicity, the glycopolymers were marked as p(AAPBAa-*r*-MAGAb) in which letters "a" and "b" represent the feed molar ratio of the copolymerization reaction (Table 1).

2.5. Characterization of the Glycopolymers. FT-IR spectrum was recorded on a Fourier Transform Infrared Spectrometer (Bio-Rad FTS-6000) using a KBr tablet containing glycopolymer powders at a resolution of 8 cm^{-1}. Proton nuclear magnetic resonance (^{1}H NMR) spectra were recorded at room temperature using a Varian Unity-plus 400 NMR spectrometer. The solvent was dimethyl-d_6 sulfoxide with three drops of D_2O. The thermogravimetric analysis of the glycopolymers, using 3−5 mg per sample, was conducted in nitrogen, at a heating rate of 10 °C/min, using a thermogravimetric analyzer (TGA; TG 209, NETZSCH).

2.6. Preparation of the NPs. NPs were prepared using the nanoprecipitation method.[50,51] In brief, 15 mg of amphiphilic glycopolymer was dissolved in 3 mL of a mixed solvent of dimethyl sulfoxide (DMSO) and H_2O (1:1, v/v) and 20 mL of distilled water was added dropwise to the solution under magnetic stirring. The procedure yielded an opalescent suspension and the solution was incubated overnight at room temperature with continuous stirring. The resulting NPs were transferred to a dialysis tube (MWCO 3500) and dialyzed in sufficient deionized water with rapid stirring for 24 h. To remove the organic solvent, the deionized water was changed every 3 h. The nanoparticle

solution was then centrifuged at 17000 × *g* for 30 min. The supernatant was carefully poured away to avoid stirring the precipitate. To prepare insulin-loaded NPs, 10 mg of insulin was dissolved in 20 mL of distilled water and was slowly added to the glycopolymer solution. The resulting insulin-glycopolymer solution was then prepared as described for the empty NPs. Finally, the precipitate was washed with deionized water and centrifuged three times prior to lyophilization of the precipitate.

2.7. Characterization of the NPs. The hydrodynamic diameter (D_H) and size distribution of the NPs, before and after treatment with 1 mg/mL or 3 mg/mL of glucose, were determined by dynamic light scattering (DLS) using a laser light scattering spectrometer (BI-200SM) equipped with a digital correlator (BI-9000AT). These measurements were carried out at 37 °C in phosphate buffer solution (PBS), pH 7.4, with the exception of one array of samples, which were analyzed at various pH values (pH 6.0, 7.4, and 8.0). The NPs were exposed to a polarized argon laser (λ = 636 nm) and the refraction was measured at 90°. Measurements were collected on an autocorrelator and analyzed using the Brookhaven software provided by the manufacturer. The morphological characteristics of the NPs before and after glucose treatment were determined by transmission electron microscopy (TEM, Philips EM400ST). Samples were placed on copper grids coated with Formvar films for viewing with the TEM.

2.8. Reversible Glucose Sensitivity of the NPs. p(AAPBA2-*r*-MAGA1) NPs were chosen as the representative nanoparticle to study the reversible glucose sensitivity of the glycopolymers. The empty p(AAPBA2-*r*-MAGA1) NPs were treated with 3 mg/mL glucose in PBS (pH 7.4) for 8 h prior to dialysis for 24 h. Following dialysis, the NPs in the dialysis tube were then exposed to 3 mg/mL glucose. The size of the NPs was monitored by DLS.

2.9. Evaluation of the Insulin-Loading Capacity of the NPs. The entrapment efficiency of insulin was determined after isolation of the NPs from the nanoparticle solution containing free insulin, which was achieved by three cycles of dispersion-recentrifugation (17000 × *g*, 30 min, 20 °C). The amount of free insulin in the collected supernatant was measured by the Bradford method using a UV spectrometer (Shimadzu UV-2550) at 595 nm.[52] Insulin entrapment efficiency (EE) and loading capacity (LC) were calculated using the following equations[53−55]

$$\mathrm{EE} = \frac{\text{total insulin} - \text{free insulin}}{\text{total insulin}} \times 100$$

$$\mathrm{LC} = \frac{\text{total insulin} - \text{free insulin}}{\text{nanoparticles weight}} \times 100$$

2.10. In Vitro Release Studies. Insulin release from the glycopolymer NPs was analyzed by incubating insulin-loaded NPs at 37 °C (±0.5 °C) in PBS (pH 7.4) with different glucose concentrations (0, 1, and 3 mg/mL) while shaking (100 rev/min). Another study on insulin release from p(AAPBA2-*r*-MAGA1) NPs was conducted by changing glucose concentration from 0 mg/mL to 3 mg/mL in the same release medium. The NPs were incubated in absence of glucose in the first 12 h and then glucose was added to a concentration of 3 mg/mL. At predetermined time-points, samples were centrifuged at 17000 × *g* for 5 min and the supernatant was taken and replenished by fresh buffer solution. The amount of free insulin was determined by the Bradford method and a calibration curve was generated using nonloaded NPs to correct for the intrinsic absorption of the polymer. In each experiment, the samples were analyzed in triplicate and error bars represent the standard deviation.

2.11. Circular Dichroism Spectroscopy. The stability of the released insulin was determined by analysis of the conformation of released insulin using circular dichroism (CD) and the resulting spectrum was compared to standard insulin. The standard insulin solution was prepared in PBS (pH 7.4) to a final concentration of 0.1 mg/mL. CD measurements were performed on a Jasco J-715 CD spectropolarimeter at 25 °C with a cell length of 0.1 cm. For the far-UV CD spectra, samples were scanned from 190 to 260 nm and accumulated 10 times, at a resolution of 1.0 nm and scanning speed of 100 nm/min. All CD data are expressed as mean residue ellipticity.[56]

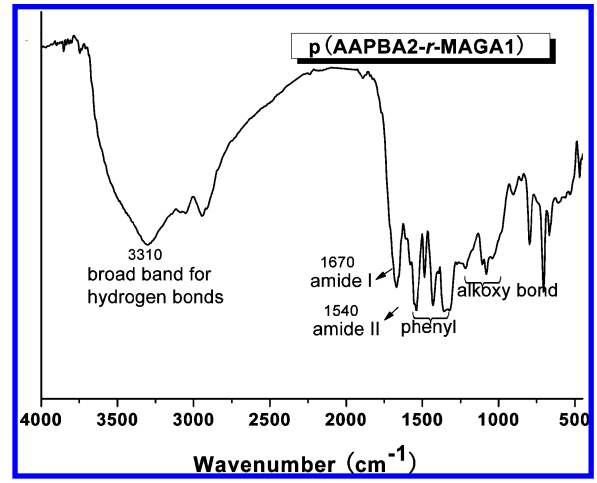

Figure 1. FT-IR spectrum of p(AAPBA2-*r*-MAGA1).

2.12. Relative Cell Proliferation Rate (RCPR). RCPR was evaluated by using NIH 3T3 cell line. The cell line was cultured in Dulbecco's modified Eagles medium (DMEM) in 5% CO_2, 95% O_2. The cells were seeded into 96-well plates at 10000 cells per well. Cells were allowed to grow to confluence for 24 h. Various glycopolymers were dissolved in a mixed solvent of DMSO and H_2O (1:1, v/v). After removal of the organic solvent by dialysis, the resulting solution was diluted with culture medium to give a final range of concentrations from 25 to 500 μg/mL. The medium from each well was replaced with 200 μL of the glycopolymer-culture medium solution. The plates were incubated at 37 °C in 5% CO_2 for 24 h. Each sample was tested in six replicates per plate. After 24 h, the culture medium and 20 μL of MTT were used to replace the mixture in each well. The cells were incubated for another 4 h in 5% CO_2 at 37 °C prior to removal of the culture medium and MTT. Isopropanol (100 μL) was added to each well to dissolve the formazan crystals that formed in response to MTT exposure. Plates were incubated in 5% CO_2 at 37 °C for 10 min and at 6 °C for 15 min prior to determination of optical density using a microplate reader at 570 nm. RCPR was determined as a percentage of the positive control: untreated cells were used as the positive control and their proliferation rate was set to 100%.

3. Results and Discussion

3.1. Characterization of the Glycopolymers. *3.1.1. FT-IR Spectroscopy.* The FT-IR spectrum (Figure 1) of p(AAPBA2-*r*-MAGA1) exhibits a broad absorption band with a range of 3200 to 3600 cm^{-1}, which was attributed to the hydrogen bonds formed between the hydroxyls of the carbohydrate moieties. The peak absorption band of 3310 cm^{-1} was due to N−H stretching. Furthermore, as a result of carboxyl formation when the maleimide ring of MAGA opened, the broad absorption band stretched to 2500 cm^{-1}. The amide I band assigned to C═O stretching resulted in an absorption band of 1670 cm^{-1}, while an absorption band at 1540 cm^{-1} was assigned to the N−H bending vibration (amide II band) of a secondary amide. The band in the 1080−1200 cm^{-1} region resulted from the C−O stretching and corresponded to the alkoxy bond in the carbohydrate moieties. Except for the broad absorption band and C−O stretching band that reflected the presence of the carbohydrate moieties, the absorption bands were typical of the phenyl ring in AAPBA at 1425, 1485, 1580, and 1600 cm^{-1}.

3.1.2. ^1H NMR Spectroscopy. Figure 2 shows the ^1H NMR spectrum of AAPBA, MAGA, and p(AAPBA2-*r*-MAGA1). The spectrum of AAPBA (Figure 2a) was characterized as follows:

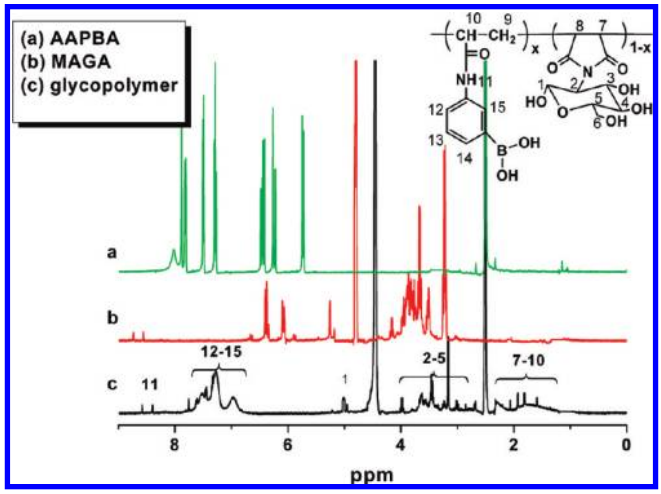

Figure 2. ^{1}H NMR spectra (400 MHz). (a) AAPBA in DMSO-d_6, (b) MAGA in D_2O, and (c) p(AAPBA2-*r*-MAGA1) in the mixed solvent of DMSO-d_6 and D_2O.

^{1}H NMR (DMSO-d_6): δ 5.8, 6.2 (2H, CH_2), 6.4 (1H, CH), 7.3, 7.5, 7.8, 7.9 (4H, Ar−H), 10.1 (1H, NH). In the ^{1}H NMR (D_2O) spectrum of MAGA (Figure 2b), protons from the double bond gave peaks at 6.1 and 6.4 ppm. The peak at 5.2 ppm refers to the proton on the anomeric carbon of the sugar residue and a broad multiplet from 3.3 to 4.3 ppm, which was assigned to other protons on the sugar residue, was also observed.[57,58] Compared with the spectra of the monomers AAPBA and MAGA, it was obvious in the spectrum of p(AAPBA2-*r*-MAGA1) that peaks of the ethylene group disappeared and the protons in the newly formed main chain generated peaks from 1.1 to 2.3 ppm.[59] It is important to note that both typical peaks of the phenyl and sugar residue were preserved in the glycopolymers. The protons of the phenyl group resulted in peaks between 7.0 and 8.0 ppm, while the proton on the anomeric carbon of the sugar residue generated a peak near 5.0 ppm. The approximate copolymer composition was calculated using the ^{1}H NMR integral intensity of the signal between the 4H, phenyl moiety (7.0−8.0 ppm), and 1H, anomeric carbon of the sugar moiety (5.0 ppm).[40] The results of the copolymerization are shown in Table 1. The mole proportion of AAPBA in the glycopolymers increased in correlation with the feed mole ratio. Furthermore, all glycopolymers contained a larger AAPBA content than the corresponding molar ratio of AAPBA to MAGA used for the polymerization, which was due to the higher solubility of AAPBA in the reaction medium and the higher reactivity ratio of AAPBA compared to MAGA.[60] The yields for each copolymerization were 50−58%.

3.1.3. Thermal Analysis. Thermogravimetric (TG) and derivative thermogravimetric (DTG) curves for the glycopolymers are shown in Figure 3. It can be seen from the DTG curves (Figure 3B) that there were three distinct degradations at 70, 260, and 375 °C. The first degradation, with a weight loss of 7%, was assigned to free water and to water linked by hydrogen bonds, which were released at 20−130 °C and reached a maximum at 70 °C. The second degradation, which was maximized around 260 °C, corresponded to the thermal decomposition of the pendant sugar residue.[38,43] As the content of MAGA in the glycopolymer increased, (p(AAPBA4-*r*-MAGA1) < p(AAPBA2-*r*-MAGA1) < p(AAPBA1-*r*-MAGA1)), decomposition was most prevalent, although the resulting change in glycopolymer weight was minimal. At temperatures up to 330 °C, the decreases in the weights of the polymers p(AAPBA4-*r*-MAGA1), p(AAPBA2-*r*-MAGA1), and p(AAPBA1-*r*-MAGA1) were 16, 17, and 19%, respectively. The last stage of thermal degradation, occurring between 330 and 480 °C, displayed peaks with a maximum value of 375 °C and was assigned to the thermal degradation of the backbone.[58,61] At this stage, the decrease in polymer weight was approximately 60%. The changes in polymer weight were calculated from the thermogravimetric curves displayed in Figure 3A.

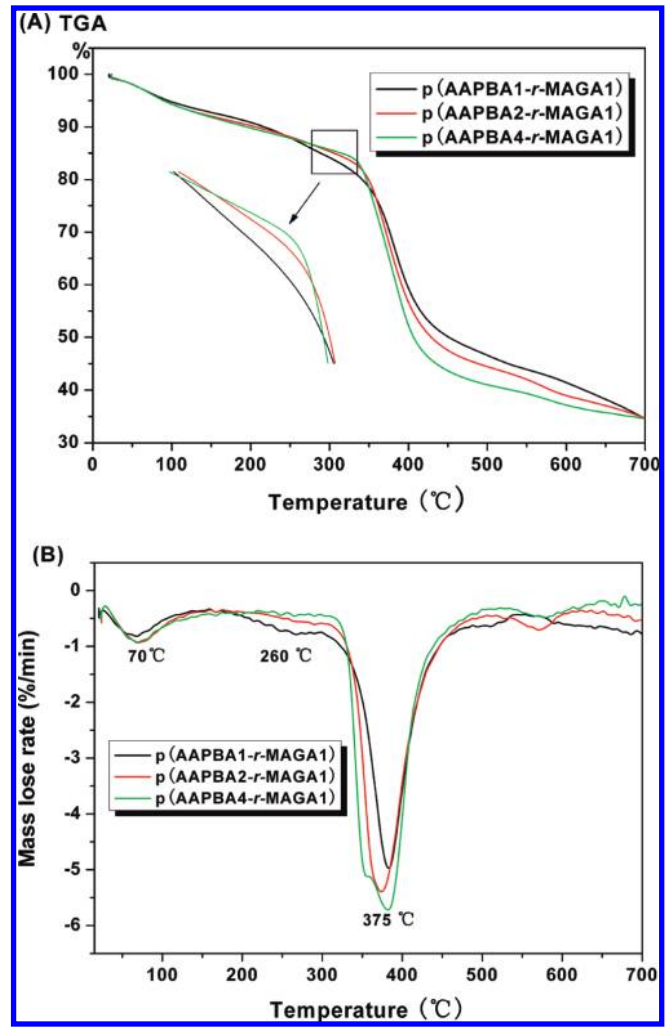

Figure 3. Thermal analysis of glycopolymers. TG (A) and DTG (B) curves for p(AAPBA1-*r*-MAGA1) (black), p(AAPBA2-*r*-MAGA1) (red), and p(AAPBA4-*r*-MAGA1) (green).

3.2. Self-Assembly and Characterization of the NPs. Because of the ill-defined structure and broad polydispersity of random copolymers, little has been exploited of their assemblies in aqueous solution. However, Tian et al.[46] described photoresponsive, amphiphilic, random copolymers that self-assembled to nanoaggregates. These copolymers underwent continuous morphological transitions, changing from spherical micelles to hollow tubes and wormlike rods to large vesicles. In the current study, the amphiphilic, random glycopolymers synthesized also self-assembled to NPs using the nanoprecipitation method, which was similar to the process described by Tian et al. In addition to the intrinsic amphiphilicity, the complexation of AAPBA with the glucosamine moieties in MAGA also promoted the glycopolymer self-assembly (Scheme 2a). Shiomi et al.[62,63] demonstrated that a glucose molecule can complex with two boronic acids at its 4-OH, 5-CH_2OH besides 1,2-diols. Therefore, the 4-OH, 5-CH_2OH of glucosamine can bind with AAPBA, leading to inter- or intramolecular interaction. The morphology and size of the NPs were determined by TEM and

Scheme 2. Self-Assembly of the Glycopolymers without/with Insulin and Glucose-Sensitive Release

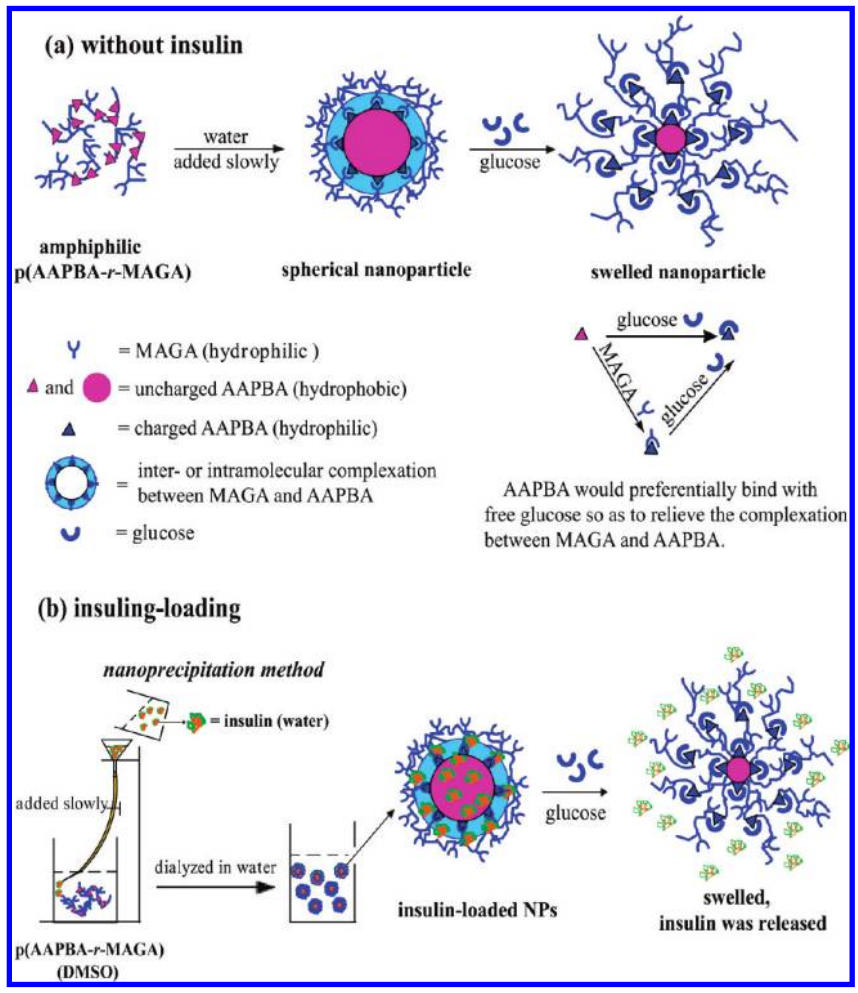

DLS. TEM analysis of p(AAPBA1-*r*-MAGA1) NPs (Figure 4A) clearly demonstrated that the NPs are well dispersed as individual particles, with a spherical shape and a size of approximately 40 nm. D_H of the empty NPs is shown in Figure 5 (red histogram). Generally speaking, all three types of NPs were 120−200 nm and exhibited a narrow size distribution, with a polydispersity index (PDI) between 0.112 and 0.128. The average D_H for the NPs p(AAPBA1-*r*-MAGA1), p(AAPBA2-*r*-MAGA1), and p(AAPBA4-*r*-MAGA1) were 123.0, 180.6, and 154.2 nm, respectively.

3.3. Swelling of the NPs Treated with Glucose and the Glucose Sensitivity. The introduction of AAPBA group made the resulting NPs glucose-sensitive. As seen in Figure 4B, after treatment with 3 mg/mL glucose, the p(AAPBA1-*r*-MAGA1) NPs swelled to nearly 60 nm in size. Notably, after glucose treatment, the NPs had a compact core surrounded by a fluffy coat. Both the swelling and the fluffy coat suggest that glucose exposure can alter the morphology of the NPs and that these glycopolymers are sensitive to glucose. Table 2 lists D_H values and PDI of the NPs in PBS of pH 7.4 with different glucose concentrations at 37 °C. Even after glucose treatment, there was a narrow size distribution, with the PDI ranging from 0.071 to 0.153 for all samples analyzed. This was in accordance with the dispersion seen by TEM analysis (Figure 4). The NPs swelled gradually as the glucose concentration increased from 0 to 3 mg/mL, which correlated to the glucose-sensitivity of the AAPBA moieties in the glycopolymer. The increase in the size of the NPs was in the order of p(AAPBA1-*r*-MAGA1) > p(AAPBA2-*r*-MAGA1) > p(AAPBA4-*r*-MAGA1). The charge interaction between the amide group and boronic acid can promote polymer shrinking rather than swelling.[64] Specifically, the charge interaction between the amide group in MAGA and boronic acid would stabilize the anionic nature of glucose-bound boron, thereby reducing the electrostatic repulsion and solvation by water that would lead to swelling. The less MAGA the glycopolymer contained, the less charge interaction between the amide group and boronic acid, increasing the amount of nanoparticle swelling. However, according to Shiino et al.,[65] the amino group present in the AAPBA polymer could enhance the stability of the boronic acid−polyol complex and lower the pH value at which the polymer responds to glucose. In the glycopolymers synthesized, MAGA and the amide group in MAGA next to AAPBA may play a similar role and, thereby, enhance the glucose sensitivity of the polymers at a physiological pH. In the current study, we measured the D_H of p(AAPBA2-*r*-MAGA1) NPs after treatment with 3 mg/mL of glucose in PBS at various pH values (6.0, 7.4, and 8.0) by DLS (Table 2). The D_H value for p(AAPBA2-*r*-MAGA1) was 182.4 nm at pH 6.0, which was minimally different compared to the D_H value without glucose (180.6 nm). However, at a physiological pH (pH = 7.4), the NPs swelled from 180.6 to 211.7 nm, which was similar to the response seen at pH 8.0 (218.6 nm), indirectly suggesting an effect of MAGA on enhancing the glucose sensitivity at physiological pH. The enhancement of glucose responsiveness should decrease as the content of MAGA in p(AAPBA1-*r*-MAGA1), p(AAPBA2-*r*-MAGA1), and p(AAPBA4-*r*-MAGA1) decreases gradually. Furthermore, Alexeev et al.[66−68] reported that glucose could form a bis-bidentate complex

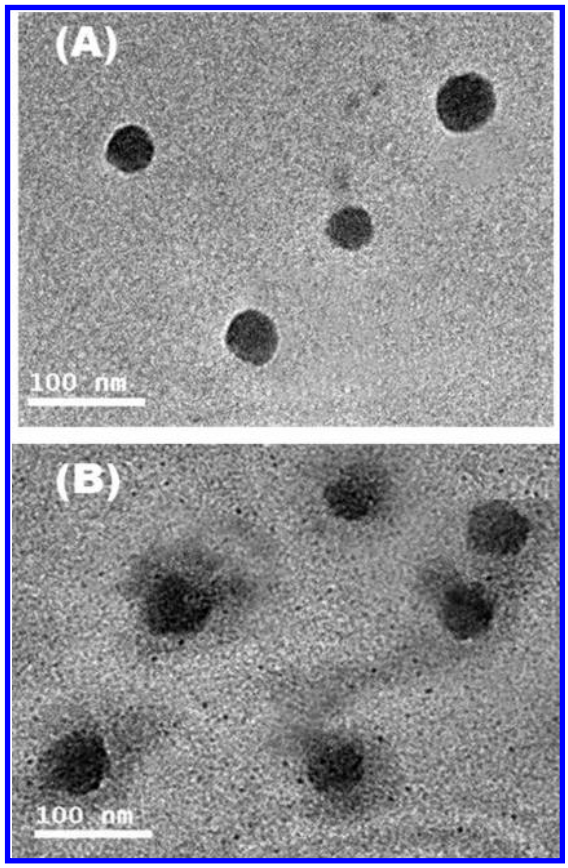

Figure 4. TEM of p(AAPBA1-*r*-MAGA1) NPs before (A) and after (B) treatment with 3 mg/mL glucose.

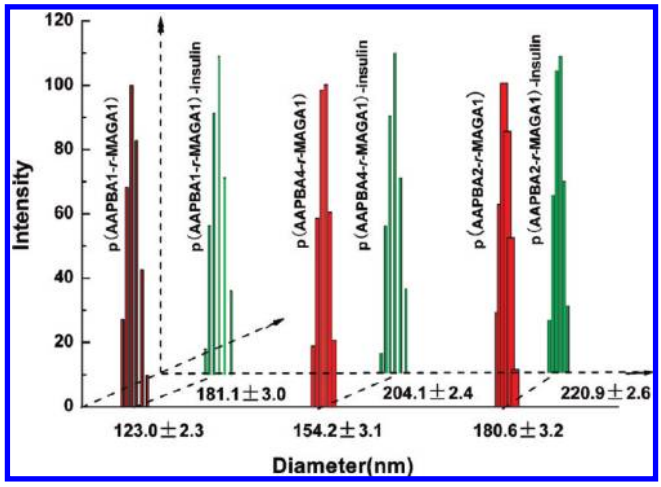

Figure 5. D_H and size distribution (DLS) of the NPs and insulin-loaded NPs.

with boronic acid derivatives. Owing to the bidentate binding of glucose by two boronic acid moieties, the glucose molecule can act as a cross-linker that does not promote swelling. Therefore, as the AAPBA content increased in order of p(AAPBA1-*r*-MAGA1) < p(AAPBA2-*r*-MAGA1) < p(AAPBA4-*r*-MAGA1), more glucose-mediated cross-linking occurred and the swelling tendency of the NPs decreased.

3.4. Reversible Glucose Sensitivity of the NPs. The result of DLS monitoring showed that the glycopolymers exhibited reversible glucose sensitivity (Figure 6). The sample swelled from 180.6 to 211.7 nm after the first glucose treatment and then contracted to 181.5 nm, which was near its original size, after dialyzing against deionized water for 24 h. When treated with glucose for the second time, the NPs swelled to 205.8 nm.

3.5. Insulin-Loading of the NPs. *3.5.1. Insulin-Loading and Size of Insulin-Loaded NPs.* Table 3 shows EE and LC of insulin in the glycopolymer NPs. Both the EE and LC for each of the three glycopolymer NPs were increased in the following order: p(AAPBA2-*r*-MAGA1) < p(AAPBA4-*r*-MAGA1) < p(AAPBA1-*r*-MAGA1). They did not increase with increasing hydrophilic MAGA content or with a higher content of hydrophobic AAPBA. The green histograms in Figure 5 show the size and distribution of insulin-loaded NPs, which are labeled as p(AAPBAa-*r*-MAGAb)-insulin. These results demonstrate that the size of the insulin-loaded NPs was greater than that of empty NPs. Moreover, the insulin-loaded NPs maintained a narrow distribution, with a PDI between 0.071 and 0.112. The size increments after loading with insulin, which can be calculated from the data seen in Figure 5, were 58.1, 40.3, and 49.9 nm for p(AAPBA1-*r*-MAGA1), p(AAPBA2-*r*-MAGA1), and p(AAPBA4-*r*-MAGA1), respectively. They are in a similar order as for EE and LC for each glycopolymer.

Additionally, the impact of glucose treatment on insulin-loaded NPs was also examined using insulin-loaded p(AAPBA2-*r*-MAGA1) NPs as a representative particle (Table 2). The NPs swelled in correlation with increasing glucose concentration, and maintained a narrow size distribution of 0.071−0.102. The swelling behavior of the insulin-loaded NPs was comparable to that of the empty p(AAPBA2-*r*-MAGA1) NPs.

3.5.2. Self-Assembly of the Glycopolymer with Insulin and Glucose-Sensitive Swelling. Insulin was dissolved in the water phase during the nanoprecipitation procedure and added, dropwise, to the glycopolymer solution (Scheme 2b). Proteins with both random sequenced hydrophilic and hydrophobic amino acids in the linear chain often associate to form stable complexes.[69−71] Therefore, we anticipate that insulin should interact and self-assemble with the amphiphilic glycopolymers due to both hydrophilic and hydrophobic interactions. Scheme 2b illustrates the formation of the insulin-loaded NPs. Additionally, the complexation of AAPBA and the glucosamine moieties on MAGA is another force to be considered for self-assembly of the glycopolymers. However, the interaction between MAGA and AAPBA is not as strong as between free glucose and AAPBA. When the NPs were treated with free glucose, AAPBA would preferentially bind free glucose so as to relieve the complexation between MAGA and AAPBA. The introduction of glucose also increases the charged phenylborates, thus enhancing the hydrophilicity of the NPs and promoting NPs swelling.

3.6. In Vitro Release Profile of Insulin upon Exposure to Glucose. Figure 7 shows the cumulative release profiles of insulin from the insulin-loaded p(AAPBA2-*r*-MAGA1) NPs in response to different concentrations of glucose. The cumulative release percentage was the sum of the amount of released insulin at a specific time divided by the amount of insulin loaded in the NPs sample. Within the first 2 h of glucose treatment, the release profile indicated a burst release phase for all glucose concentrations examined. After the first couple of hours, insulin was gradually released from the loaded NPs (Figure 7a−c). The burst release in medium without glucose indicated that some of the insulin was adsorbed onto the surface during preparation of the NPs and, then, diffused rapidly when NPs came into contact with the release medium. In medium containing glucose, this burst of insulin was much higher, with 34 and 50% of the insulin being released into the medium following treatment with 1 and 3 mg/mL of glucose concentration, respectively, compared to 16% insulin release in NPs incubated in glucose-free medium. Another study on release profiles of p(AAPBA2-*r*-MAGA1)

Table 2. D_H and PDI of the NPs at Various Glucose Concentrations Measured by DLS

glucose concentration	p(AAPBA1-*r*-MAGA1)		p(AAPBA2-*r*-MAGA1)		p(AAPBA4-*r*-MAGA1)		p(AAPBA2-*r*-MAGA1)-insulin[a]	
	D_H(nm)	PDI	D_H(nm)	PDI	D_H(nm)	PDI	D_H(nm)	PDI
0 (mg/mL)	123.0 ± 2.3	0.121 ± 0.012	180.6 ± 3.2	0.128 ± 0.010	154.2 ± 3.1	0.112 ± 0.009	220.9 ± 2.6	0.071 ± 0.013
1 (mg/mL)	142.7 ± 3.5	0.132 ± 0.008	196.5 ± 4.4	0.133 ± 0.006	163.5 ± 2.9	0.119 ± 0.013	235.4 ± 2.8	0.085 ± 0.009
3 (mg/mL)	163.5 ± 2.8	0.146 ± 0.009	211.7 ± 3.6	0.153 ± 0.011	170.2 ± 3.4	0.126 ± 0.020	248.2 ± 1.9	0.102 ± 0.012
			182.4 ± 3.9[b]	0.137 ± 0.013				
			218.6 ± 2.7[c]	0.146 ± 0.008				

[a] Insulin-loaded p(AAPBA2-*r*-MAGA1) NPs were chosen as a representative to investigate the size increase of insulin-loaded NPs with increasing glucose concentration. [b] Measured in PBS, pH 6.0 with 3 mg/mL glucose. [c] Measured in PBS, pH 8.0 with 3 mg/mL glucose.

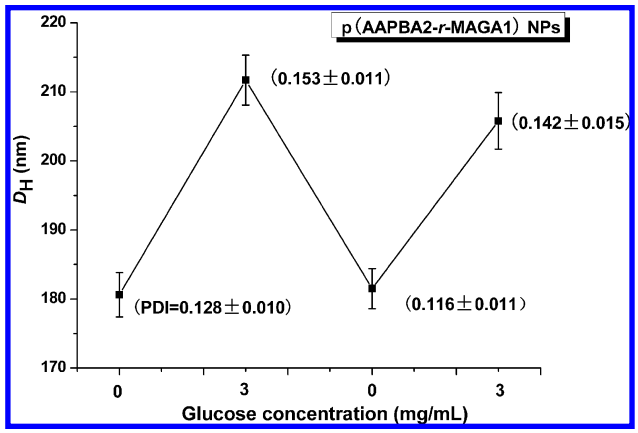

Figure 6. Reversible glucose sensitivity of p(AAPBA2-*r*-MAGA1) NPs.

Table 3. EE and LC of the Glycopolymer NPs

sample	EE (%)	LC (%)
p(AAPBA1-*r*-MAGA1)	80.15 ± 1.25	11.44 ± 0.39
p(AAPBA2-*r*-MAGA1)	62.64 ± 2.89	9.58 ± 0.24
p(AAPBA4-*r*-MAGA1)	72.37 ± 3.44	10.22 ± 0.35

NPs was conducted by changing the glucose concentration from 0 to 3 mg/mL in the same release medium. The NPs were incubated in absence of glucose for the first 12 h. After the percent of insulin released reached a plateau, glucose was added to a concentration of 3 mg/mL (Figure 7d). There were two burst releases, as expected, in the two distinct stages: one burst occurred without glucose and was for normal diffusion-based release, while the other was for glucose-sensitive release. For

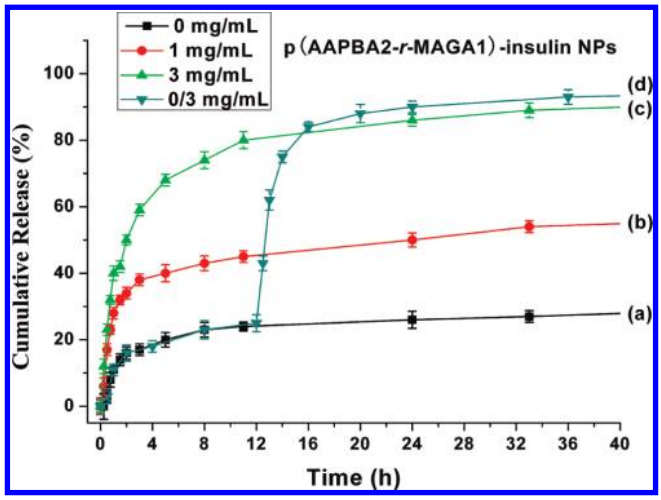

Figure 7. In vitro cumulative release of insulin from p(AAPBA2-*r*-MAGA1) NPs at various glucose concentrations: (a) medium only, (b) 1 mg/mL, (c) 3 mg/mL, and (d) medium only for the first 12 h and then 3 mg/mL.

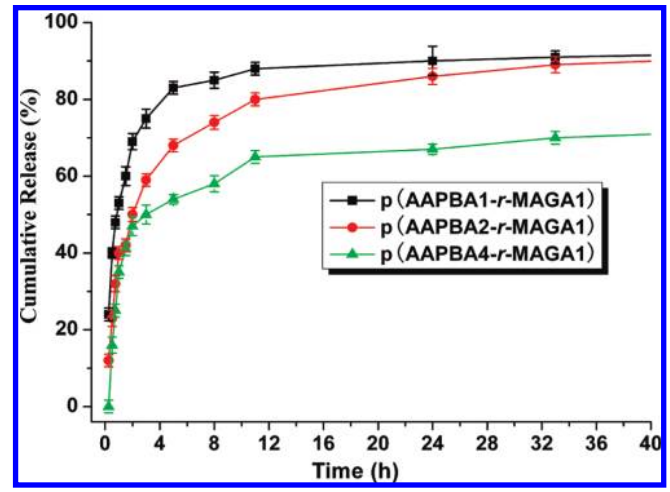

Figure 8. In vitro cumulative release of insulin from different p(AAPBA-*r*-MAGA) NPs at a glucose concentration of 3 mg/mL.

the curves in Figure 7a−c, the rate of insulin release was decreased after several hours and was nearly equal at all glucose concentrations in the later monitoring time. The amounts of insulin released after 33 h for each glucose concentration were 27, 54, and 89%, respectively. Obviously, the initial burst release of insulin and the final amount of insulin released from the glycopolymer NPs were affected by the glucose concentration. These results combined with the fact that the size of p(AAPBA2-*r*-MAGA 1)-insulin NPs increased in correlation with the glucose concentration (Table 2) suggested that the glycopolymer was responsive to glucose and released insulin rapidly upon exposure to glucose.

Figure 8 shows the release profile of insulin from insulin-loaded NPs of all three glycopolymers in medium of the same glucose concentration (3 mg/mL). The burst release of insulin occurred within the first 2 h for each glycopolymer NPs. Insulin was released rapidly from the NPs in the first 8 h in the following order: p(AAPBA1-*r*-MAGA1) > p(AAPBA2-*r*-MAGA1) > p(AAPBA4-*r*-MAGA1). The cumulative amounts of insulin released for each glycopolymer NP was 85, 74, and 58%, respectively. As discussed above, the size increase of the NPs following glucose treatment was in the order of p(AAPBA1-*r*-MAGA1) > p(AAPBA2-*r*-MAGA1) > p(AAPBA4-*r*-MAGA1). The insulin-loaded NPs became swelled after glucose exposure, which resulted in a rapid release of insulin. The glucose sensitivity of the NPs is attributed to the AAPBA component complexing with glucose. However, MAGA content can also enhance the glucose sensitivity at physiological pH. Furthermore, the greater the concentration of hydrophilic MAGA a glycopolymer contains, the easier it is for the glucose solution to access and penetrate the NPs and react with AAPBA. Therefore, the combined action of all these factors results in a release rate of insulin in the following order: p(AAPBA1-*r*-MAGA1) > p(AAPBA2-*r*-MAGA1) > p(AAPBA4-*r*-MAGA1).

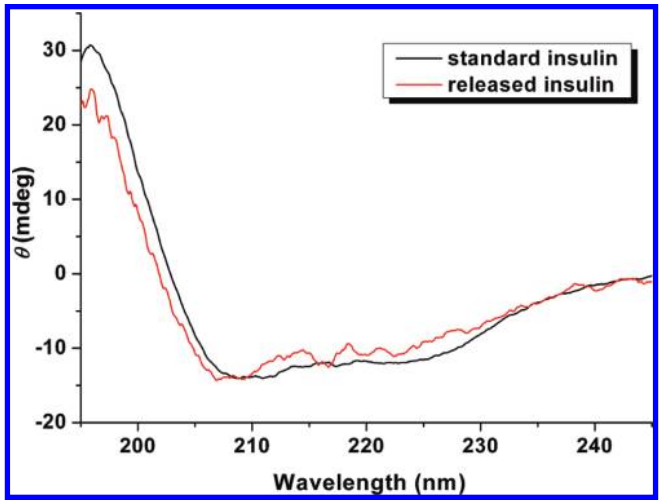

Figure 9. UV-CD spectra of standard insulin and released insulin.

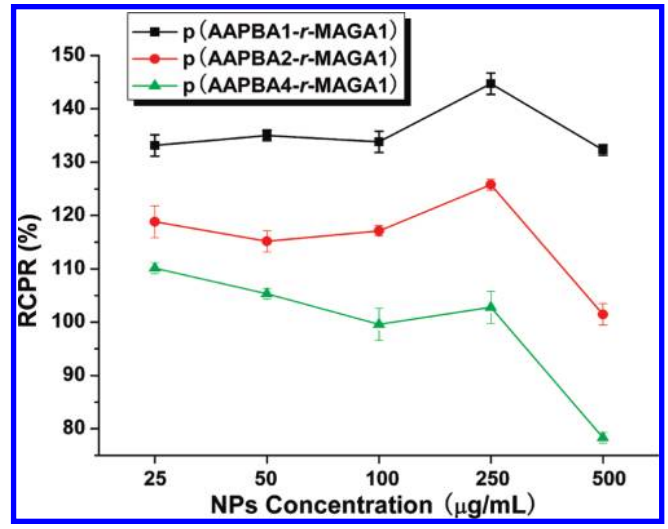

Figure 10. RCPR after incubation as a function of NPs concentration by MTT assay.

3.7. Stability of the Released Insulin. CD spectroscopy was used to evaluate the conformational changes in insulin.[72,73] The far-UV-CD band at 208 nm primarily arises from α-helix structure, while that at 223 nm is for the β-structure. The ratio between both bands ($[\Phi]_{208}/[\Phi]_{223}$) can be used to generate a qualitative measure of the overall conformational structure of insulin. In our study, the $[\Phi]_{208}/[\Phi]_{223}$ ratio for standard insulin and released insulin was 1.29 and 1.14, respectively. As indicated by the CD spectra (Figure 9), no significant conformational change was observed for the insulin released from the NPs at pH 7.4 in comparison with the standard insulin. Furthermore, the spectral characteristics indicate that the tertiary structure of released insulin has not been distorted.

3.8. Relative Cell Proliferation Rate. As described in the study by Qureshi et al.,[31] most of the boronated moieties and their derivatives have cytotoxic activity in multiple cell lines, and little is known about the cytotoxic potential of boronic acid. Therefore, in this study, it was important to verify the innocuous nature of the polymerized carbohydrate moieties present in the p(AAPBA-*r*-MAGA) copolymers. To evaluate the potential toxicity of these copolymers, in vitro cytotoxicity assays, using the p(AAPBA-*r*-MAGA) copolymers and the NIH 3T3 fibroblast cell line, were performed and analyzed by the MTT method (Figure 10). The cells were exposed to various concentrations of the glycopolymer nanoparticle solutions and incubated for 24 h. For nearly all of the cultures, the relative cell proliferation rates (RCPR) ranged from 98 to 145%, irrespective of glycopolymer NPs concentration, suggesting that the presence of the glycopolymer did not negatively impact cell proliferation. Furthermore, the RCPR increased as the number of carbohydrate moieties in the glycopolymer increased (p(AAPBA4-*r*-MAGA1) < AAPBA2-*r*-MAGA1) < (AAPBA1-*r*-MAGA1)). Because p(AAPBA4-*r*-MAGA1) contained the most AAPBA, there was a point where RCPR was lower than 80% on the curve of p(AAPBA4-*r*-MAGA1) for the highest concentration tested. Overall, the results suggest that the carbohydrate moieties might enhance the biocompatibility of the glycopolymers containing boronic acid and that these polymers have the potential for in vivo use.

4. Conclusion

Amphiphilic, random glycopolymers based on phenylboronic acid were prepared using different molar ratios of AAPBA to MAGA. The random glycopolymers could self-assemble to form NPs with a narrow size distribution using the nanoprecipitation method. TEM showed that the NPs were well dispersed as individual particles with a spherical shape. The glycopolymer NPs were sensitive to glucose and increased in size in correlation with the glucose concentration. In addition, the glucose sensitivity of the glycopolymer NPs was reversible. Insulin could be loaded into the glycopolymer NPs due to both hydrophilic and hydrophobic interactions, with a loading capacity of approximately 10%. Insulin release profiles revealed that the release of insulin was in correlation with the increasing glucose concentration. The biocompatibility of the NPs was enhanced through introduction of carbohydrate moieties, which partly resolved the issue of cytotoxicity common with phenylboronic acid. In conclusion, the data suggests that the glycopolymers may have potential for use in a self-regulated insulin delivery system in the future.

Acknowledgment. This work was supported in part by the National Natural Science Foundation of China (Grant No. 20804021), the Natural Science Foundation of Tianjin (Grant No. 08JCYBJC00300), and the Ph.D. Programs Foundation for New Teachers of Ministry of Education of China (Grant No. 200800551030).

References and Notes

(1) Qiu, Y.; Park, K. *Adv. Drug Delivery Rev.* **2001**, *53*, 321–339.
(2) Lee, W.; Hsu, C. *J. Appl. Polym. Sci.* **1999**, *74*, 3242–3253.
(3) Zhang, J.; Peppas, N. A. *Macromolecules* **2000**, *33*, 102–107.
(4) Zhao, B.; Moore, J. S. *Langmuir* **2001**, *17*, 4758–4763.
(5) Sayil, C.; Okay, O. *J. Appl. Polym. Sci.* **2002**, *83*, 1228–1232.
(6) Akala, E. O.; Kopeckova, P.; Kopecek, J. *Biomaterials* **1998**, *19*, 1037–1047.
(7) Torres-Lugo, M.; Peppas, N. A. *Macromolecules* **1999**, *32*, 6646–6651.
(8) Hirokawa, Y.; Tanaka, T. *J. Chem. Phys.* **1984**, *81*, 6379–6380.
(9) Okano, T.; Bae, Y. H.; Jacobs, H.; Kim, S. W. *J. Controlled Release* **1990**, *11*, 255–265.
(10) Gotoh, T.; Nakatani, Y.; Sakohara, S. J. *J. Appl. Polym. Sci.* **1998**, *69*, 895–906.
(11) Suzuki, A.; Tanaka, T. *Nature* **1990**, *346*, 345–347.
(12) Horkay, F.; Tasaki, I.; Basser, P. J. *Biomacromolecules* **2000**, *1*, 84–90.
(13) Wang, G.; Tian, W. J.; Huang, J. P. *J. Phys. Chem. B* **2006**, *110*, 10738–10745.
(14) Ivanov, A. E.; Larsson, H.; Galaev, I. Y.; Mattiasson, B. *Polymer* **2004**, *45*, 2495–2505.
(15) De Geest, B. G.; Jonas, A. M.; Demeester, J.; De Smedt, S. C. *Langmuir* **2006**, *22*, 5070–5074.

(16) Kikuchi, A.; Suzuki, K.; Okabayashi, O.; Hoshino, H.; Kataoka, K.; Sakurai, Y.; Okano, T. *Anal. Chem.* **1996**, *68*, 823–828.
(17) Matsumoto, A.; Yoshida, R.; Kataoka, K. *Biomacromolecules* **2004**, *5*, 1038–1045.
(18) Phillips, M. D.; James, T. D. *J. Fluoresc.* **2004**, *14*, 549–559.
(19) Horgan, A. M.; Marshall, A. J.; Kew, S. J.; Dean, K. E. S.; Creasey, C. D.; Kabilan, S. *Biosens. Bioelectron.* **2006**, *21*, 1838–1845.
(20) Cannizzo, C.; Amigoni-Gerbier, S.; Larpent, C. *Polymer* **2005**, *46*, 1269–1276.
(21) Liu, J. T.; Chen, L. Y.; Shih, M. C.; Chang, Y.; Chen, W. Y. *Anal. Biochem.* **2008**, *375*, 90–96.
(22) Kuzimenkova, M. V.; Ivanov, A. E.; Thammakhet, C.; Mikhalovska, L. I.; Galaev, I. Y.; Thavarungkul, P.; Kanatharana, P.; Mattiasson, B. *Polymer* **2008**, *49*, 1444–1454.
(23) Kataoka, K.; Miyazaki, H.; Okano, T.; Sakurai, Y. *Macromolecules* **1994**, *27*, 1061–1062.
(24) Hoare, T.; Pelton, R. *Macromolecules* **2007**, *40*, 670–678.
(25) Hoare, T.; Pelton, R. *Biomacromolecules* **2008**, *9*, 733–740.
(26) Lapeyre, V.; Gosse, I.; Chevreux, S.; Ravaine, V. *Biomacromolecules* **2006**, *7*, 3356–3363.
(27) Lapeyre, V.; Ancla, C.; Catargi, B.; Ravaine, V. *J. Colloid Interface Sci.* **2008**, *327*, 316–323.
(28) Zhang, Y.; Guan, Y.; Zhou, S. *Biomacromolecules* **2006**, *7*, 3196–3201.
(29) Zhang, Y.; Guan, Y.; Zhou, S. *Biomacromolecules* **2007**, *8*, 3842–3847.
(30) Achanta, G.; Modzelewska, A.; Feng, L.; Khan, S. R.; Huang, P. *Mol. Pharmacol.* **2006**, *70*, 426–433.
(31) Qureshi, S.; Al-Shabanah, O. A.; Al-Harbi, M. M.; Al-Bekairi, A. M.; Raza, M. *Toxicology* **2001**, *165*, 1–11.
(32) Finkelstein, J. *Nature* **2007**, *446*, 999.
(33) Seeberger, P. H.; Werz, D. B. *Nature* **2007**, *446*, 1046–1051.
(34) Lis, H.; Sharon, N. *Chem. Rev.* **1998**, *98*, 637–674.
(35) Drouillat, B.; Hillery, A. M.; Dekany, G.; Falconer, R.; Wright, K.; Toth, I. *J. Pharm. Sci.* **1998**, *87*, 25–30.
(36) Miura, Y. *J. Polym. Sci., Part A: Polym. Chem.* **2007**, *45*, 5031–5036.
(37) Muthukrishnan, S.; Zhang, M. F.; Burkhardt, M.; Drechsler, M.; Mori, H.; Muller, A. H. E. *Macromolecules* **2005**, *38*, 7926–7934.
(38) Xiao, N. Y.; Li, A. L.; Liang, H.; Lu, J. *Macromolecules* **2008**, *41*, 2374–2380.
(39) Yang, Q.; Xu, Z. K.; Dai, Z. W.; Wang, J. L.; Ulbricht, M. *Chem. Mater.* **2005**, *17*, 3050–3058.
(40) Xu, Z. K.; Kou, R. Q.; Liu, Z. M.; Nie, F. Q.; Xu, Y. Y. *Macromolecules* **2003**, *36*, 2441–2447.
(41) Ladmiral, V.; Melia, E.; Haddleton, D. M. *Eur. Polym. J.* **2004**, *40*, 431–449.
(42) Ohno, K.; Tsujii, Y.; Miyamoto, T.; Fukuda, T. *Macromolecules* **1998**, *31*, 1064–1069.
(43) Albertin, L.; Stenzel, M. H.; Barner-Kowollik, C.; Foster, L. J. R.; Davis, T. P. *Macromolecules* **2005**, *38*, 9075–9084.
(44) Spain, S. G.; Gibson, M. I.; Cameron, N. R. *J. Polym. Sci., Part A: Polym. Chem.* **2007**, *45*, 2059–2072.
(45) Ye, W.; Wells, S.; Desimone, J. M. *J. Polym. Sci., Part A: Polym. Chem.* **2001**, *39*, 3841–3849.
(46) Tian, F.; Yu, Y. Y.; Wang, C. C.; Yang, S. *Macromolecules* **2008**, *41*, 3385–3388.
(47) Chandran, K.; Nithya, R.; Sankaran, K.; Gopalan, A.; Ganesan, V. *Bull. Mater. Sci.* **2006**, *29*, 173–179.
(48) Lee, M. C.; Kabilan, S.; Hussain, A.; Yang, X. P.; Blyth, J.; Lowe, C. R. *Anal. Chem.* **2004**, *76*, 5748–5755.
(49) Aly, M. R. E.; Castro-Palomino, J. C.; Ibrahim, E. S. I.; El-Ashry, E. S. H.; Schmidt, R. R. *Eur. J. Org. Chem.* **1998**, *11*, 2305–2316.
(50) Peroche, S.; Degobert, G.; Putaux, J. L.; Blanchin, M. G.; Fessi, H.; Parrot-Lopez, H. *Eur. J. Pharm. Biopharm.* **2005**, *60*, 123–131.
(51) Bes, L.; Angot, S.; Limer, A.; Haddleton, D. M. *Macromolecules* **2003**, *36*, 2493–2499.
(52) Bradford, M. M. *Anal. Biochem.* **1976**, *72*, 248–254.
(53) Fernandez-Urrusuno, R.; Calvo, P.; Remunan-Lopez, C.; Vila-Jato, J. L.; Alouso, M. J. *Pharm. Res.* **1999**, *16*, 1576–1581.
(54) Amidi, M.; Romeijn, S. G.; Borchard, G.; Junginger, H. E.; Hennink, W. E.; Jiskoot, W. *J. Controlled Release* **2006**, *111*, 107–116.
(55) Grenha, A.; Seigo, B.; Remunan-Lopez, C. *Eur. J. Pharm. Sci.* **2005**, *25*, 427–437.
(56) Sato, M.; Furuike, T.; Sadamoto, R.; Fujitani, N.; Nakahara, T.; Niikura, K.; Monde, K.; Kondo, H.; Nishimura, S. I. *J. Am. Chem. Soc.* **2004**, *126*, 14013–14022.
(57) Lu, C. H.; Chen, X. S.; Xie, Z. G.; Lu, T. C.; Wang, X.; Ma, J.; Jing, X. B. *Biomacromolecules* **2006**, *7*, 1806–1810.
(58) Zhou, W. J.; Naik, S. S.; Kurth, M. J.; Hsieh, Y. L.; Krochta, J. M. *J. Polym. Sci., Part A: Polym. Chem.* **1998**, *36*, 2971–2978.
(59) Pasparakis, G.; Cockayne, A.; Alexander, C. *J. Am. Chem. Soc.* **2007**, *129*, 11014–11015.
(60) Shiomori, K.; Ivanov, A. E.; Galaev, I. Y.; Kawano, Y.; Mattiasson, B. *Macromol. Chem. Phys.* **2004**, *205*, 27–34.
(61) Zhou, W. J.; Kurth, M. J. *Macromolecules* **1999**, *32*, 5507–5513.
(62) Shiomi, Y.; Saisho, M.; Tsukagoshi, K.; Shinkai, S. *J. Chem. Soc., Perkin Trans. 1* **1993**, *17*, 2111–2117.
(63) Kondo, K.; Shiomi, Y.; Saisho, M.; Harada, T.; Shinkai, S. *Tetrahedron* **1992**, *48*, 8239–8252.
(64) Samoei, G. K.; Wang, W.; Escobedo, J. O.; Xu, X.; Schneider, H. J.; Cook, R. L.; Strongin, R. M. *Angew. Chem., Int. Ed.* **2006**, *45*, 1–5.
(65) Shiino, D.; Murata, Y.; Kubo, A.; Kim, Y. J.; Kataoka, K.; Koyama, Y.; Kikuchi, A.; Yokoyama, M.; Sakurai, Y.; Okano, T. *J. Controlled Release* **1995**, *37*, 269–276.
(66) Asher, S. A.; Alexeev, V. L.; Goponenko, A. V.; Sharma, A. C.; Lednev, I. K.; Wilcox, C. S.; Finegold, D. N. *J. Am. Chem. Soc.* **2003**, *125*, 3322–3329.
(67) Alexeev, V. L.; Sharma, A. C.; Goponenko, A. V.; Das, S.; Lednev, I. K.; Wilcox, C. S.; Finegold, D. N. *Anal. Chem.* **2003**, *75*, 2316–2323.
(68) Alexeev, V. L.; Das, S.; Finegold, D. N.; Asher, S. A. *Clin. Chem.* **2004**, *50*, 2353–2360.
(69) Ballister, E. R.; Lai, A. H.; Zuckermann, R. N.; Cheng, Y. F.; Mougous, J. D. *Proc. Natl. Acad. Sci. U.S.A.* **2008**, *105*, 3733–3738.
(70) Miller, R. A.; Presley, A. D.; Francis, M. B. *J. Am. Chem. Soc.* **2007**, *129*, 3104–3109.
(71) Scheibel, T.; Parthasarathy, R.; Sawicki, G.; Lin, X. M.; Jaeger, H.; Lindquist, S. L. *Proc. Natl. Acad. Sci. U.S.A.* **2003**, *100*, 4527–4532.
(72) Hinds, K.; Koh, J. J.; Joss, L.; Liu, F.; Baudys, M.; Kim, S. W. *Bioconjugate Chem.* **2000**, *11*, 195–201.
(73) Lee, S.; Kim, K.; Kumar, T. S.; Lee, J.; Kim, S. K.; Lee, D. Y.; Lee, Y. K.; Byun, Y. *Bioconjugate Chem.* **2005**, *16*, 615–620.

BM8010006